# Structural Selectivity of Aromatic Diamidines

Jonathan B. Chaires,*,† Jinsong Ren,‡ Donald Hamelberg,§ Arvind Kumar,§ Vandna Pandya,§ David W. Boykin,*,§ and W. David Wilson*,§

*James Graham Brown Cancer Center, Department of Medicine, Health Sciences Center, University of Louisville, 529 S. Jackson St., Louisville, Kentucky 40202, Key Laboratory of Rare Earth Chemistry and Physics, Changchun Institute of Applied Chemistry, Chinese Academy of Sciences, Changchun, Jilin 130022, China, and Department of Chemistry, Georgia State University, Atlanta, Georgia 30303*

*Received June 25, 2004*

Competition dialysis was used to study the interactions of 13 substituted aromatic diamidine compounds with 13 nucleic acid structures and sequences. The results show a striking selectivity of these compounds for the triplex structure poly dA:(poly dT)$_2$, a novel aspect of their interaction with nucleic acids not previously described. The triplex selectivity of selected compounds was confirmed by thermal denaturation studies. Triplex selectivity was found to be modulated by the location of amidine substiuents on the core phenyl−furan−phenyl ring scaffold. Molecular models were constructed to rationalize the triplex selectivity of DB359, the most selective compound in the series. Its triplex selectivity was found to arise from optimal ring stacking on base triplets, along with proper positioning of its amidine substituents to occupy the minor and the major−minor grooves of the triplex. New insights into the molecular recognition of nucleic acid structures emerged from these studies, adding to the list of available design principles for selectively targeting DNA and RNA.

## Introduction

Natural products and synthetic organic cations that bind in the DNA minor groove have proven useful as probes for evaluation of DNA molecular recognition as well as clinically useful agents in chemotherapy. The antibiotic netropsin, for example, is a dicationic amidine-guanidine natural product that has been extremely useful in characterizing the full molecular basis for DNA minor groove recognition.[1−4] Pentamidine is a synthetic diamidine dication that has been successfully used clinically for many years against parasitic microorganisms [5] and has seen increased use due to three primary factors: (i) the spread of AIDS throughout the world, (ii) the dramatic increase in microbial parasitic diseases in tropical environments, and (iii) the increase in immune-compromised transplant patients in developed countries. The biological activity of the family of aromatic diamidines, such as those in Figure 1, is correlated with their ability to interact strongly with the DNA minor groove in AT sequences with subsequent inhibition of one or more DNA-directed enzymes or control proteins.[5] Because of problems with toxicity and the lack of oral bioavailability of pentamidine and related diamidines, a major synthetic effort has gone into the search for additional compounds in this general family that have improved biological activity and bioavailability.

A furan-based diamidine called furamidine (DB75, Figure 1) is related in structure to pentamidine. Furamidine has shown very promising therapeutic activity against a variety of parasitic microorganisms.[5] Rapid cellular uptake with nuclear accumulation of this compound is clearly observed by fluorescence microscopy with the intrinsic compound fluorescence.[6] In a very promising result for the use of these compounds in human treatment, a bis-methoxamidine prodrug of DB75, which is activated to DB75 in vivo, has successfully completed phase I clinical trials. Phase II clinical trials for the treatment trypanosomal diseases and for treatment of *Pneumocystis carinii* pneumonia are proceeding, and to date the results show promising activity and low toxicity.[5]

DB75 binds strongly in the minor groove of AT DNA sequences and forms hydrogen bonds with the edges of AT base pairs at the floor of the groove.[7,8] The crescent shape of the compound matches the curvature of the minor groove receptor site in AT sequences. The compound fits snuggly into the narrow and deep minor groove of AT sequences and covers four base pairs in its DNA complex. The G-$NH_2$ group in minor groove sequences with GC base pairs sterically interferes with strong minor groove complex formation. As a result, diamidines such as DB75 bind significantly more weakly to GC than to AT DNA sequences. Interestingly, DB75 can actually switch to an intercalation rather than a minor groove binding mode in GC-containing sequences.[9] Apparently the relatively flat surface of the diphenylfuran aromatic system of DB75 can stack with GC base pairs better by intercalation than fit into the wide and sterically hindered minor groove of GC sequences.

The amidine terminal groups of DB75 contribute significantly to the DNA binding interactions through stacking with the walls of the minor groove, hydrogen bonding, and polyelectrolyte interactions.[8] Their charges

* Address correspondence regarding nucleic acids binding analysis to J.B.C., chemical synthesis to D.W.B., and molecular modeling to W.D.W. E-mail: J.B.C., jbchai01@gwise.louisville.edu; D.W.B., chedwb@panther.gsu.edu; W.D.W., chewdw@panther.gsu.edu.
† University of Louisville.
‡ Chinese Academy of Sciences.
§ Georgia State University.

10.1021/jm049491e CCC: $27.50 
Published on Web 10/02/2004

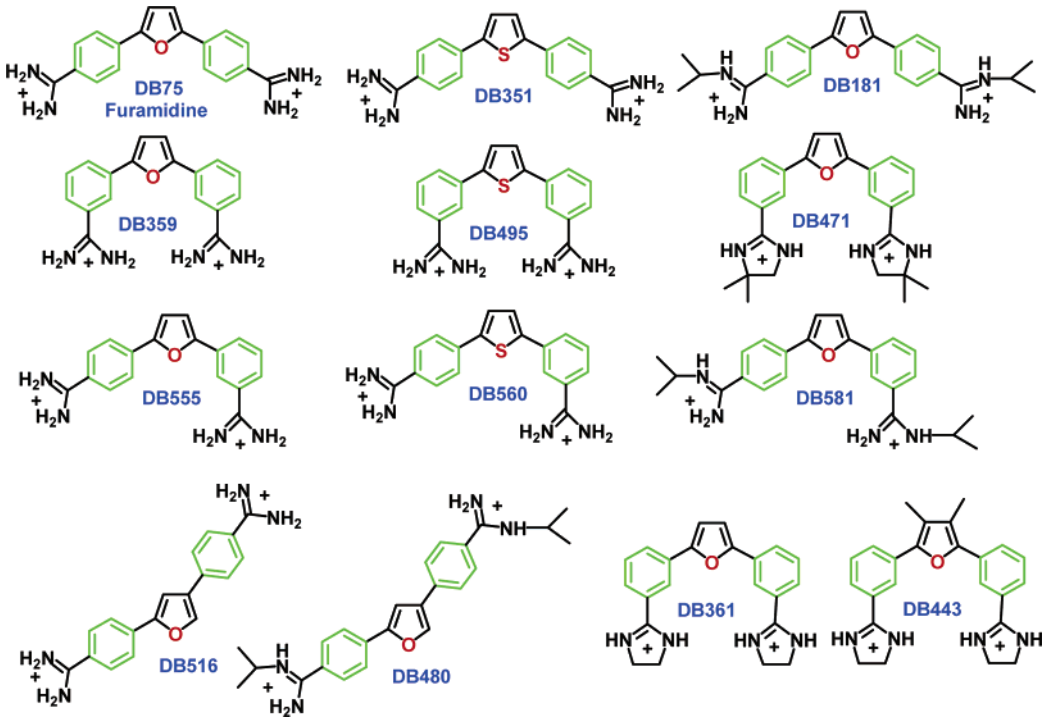


**Figure 1.** Structures of the aromatic diamidines are grouped into related sets. The top row contains the DB75 parent compound and para derivatives. The second and third rows contain meta−meta and meta−para derivatives, respectively. The left column contains isomers of DB75 that allow a rigorous test of the importance of the different structural features of the parent compound. Other isomer sets are composed of the alkyl amidines DB181, DB581, and DB480, and the thiophenes DB351, DB495 DB560. DB471, DB361, and DB443 provide a group of related cyclic amidine analogues. All compounds are substituted at the 2- and 5-positions of the central heterocycle, except for DB516 and DB480, which are substituted at the 2- and 4-positions.

drive coupled ion and (possible) water release, providing a favorable free energy contribution.[10] Replacement of the amidines with a cyclic imidazoline group increases the planarity of the overall structure and causes an enhancement of the intercalation binding mode of the compound, particularly with GC base pair containing sequences.[9] Alkylation of the amidine substituents can affect the compound−DNA interaction strength as well as the sequence preference in a manner that depends on the size and shape of the alkyl group. Introduction of a cyclopentyl or an isopropyl group on the amidine, for example, enhances DNA interactions, while more bulky groups can inhibit binding.[10]

The clinical activity of this class of compounds along with the structural information on their DNA minor groove binding mode as well as their varied and novel DNA interactions makes the compound set an ideal starting point for evaluation of interactions with a variety of DNA and RNA structures and sequences. Because of the different DNA sequence and compound structure dependent binding modes of this compound family, it is clear that within the group there could be a variety of nucleic acid interaction types and strengths that are not yet discovered. It is essential to develop a broader knowledge of the possible nucleic acid interactions of these compounds if we are to better understand their biological activity and develop additional agents against resistant organisms and diseases. An excellent method for rapid investigation of compound interactions with different nucleic acid sequences and structures is the recently developed competition dialysis method.[11−13] In the competition dialysis method, an array of nucleic acid sequences and structures is dialyzed against a common free ligand solution. More ligand accumulates in the nucleic acid sample with the preferred sequence or structure, providing a simple and direct quantitative measure of selectivity. A variety of compounds with systematic structural changes (Figure 1) were designed and synthesized to determine how modifying different parts of the DB75 structure would affect the ability of the compound to interact with a validated panel of test DNA and RNA structures and sequences.

The cationic groups of furamidine, for example, are in the para−para positions of the phenyl component, and minor groove binding is preferred in DNA complexes of this compound. Isomers with para−meta and meta−meta cationic groups (Figure 1), however, shift their binding preference to an intercalation or mixed binding mode with DNA duplexes, even with pure AT DNA sequences.[14] We have selected several different types of compounds with modified positions of the cationic groups for use in the dialysis assay. As described above, imidazoline substituents as well as alkylation of the amidine groups can also cause variations in DNA binding strength and binding mode, and we selected four types of terminal side chains, amidine, isopropyl-amidine, imidazoline, and dimethyl-imidazoline, to evaluate in detail the influence of this very important function on the nucleic acid interactions of the compounds. To probe the limits of furan substitution, the furan was converted to the thiophene heterocycle, and 2,4-substituted furan isomers were prepared to compare with the usual 2,5-substitution positions of DB75 and analogues. The competition dialysis results reported here provide a rationale to explain the relationships between sequence selectivity and mode of binding to DNA for unfused aromatic dications related to furamidine (Figure 1).

## Materials and Methods

**Materials**. The synthetic polydeoxyribonucteotides poly dT and poly dA:poly dT used in melting sudies were purchased from Amersham-Pharmacia Biotech, Inc. (Piscataway, NJ) and were used without further purification. All studies were done in BPES buffer, consisting of 6 mM $Na_2HPO_4$, 2 mM $NaH_2PO_4$, 1 mM $Na_2EDTA$, 0.185 M NaCl, pH = 7.0.

**Synthesis.** The syntheses of DB75,[15] DB181,[16] DB351,[17] DB480,[18] and DB516[18] have been previously reported. Melting points were recorded using a Thomas-Hoover (Uni-Melt) capillary melting point apparatus and are uncorrected. TLC analysis was carried out on silica gel 60 $F_{254}$ precoated aluminum sheets and detected under UV light. $^1H$ and $^{13}C$ NMR spectra were recorded by employing a Varian GX400 or Varian Unity Plus 300 spectrometer, chemical shifts (d) are in ppm relative to TMS as internal standard, and coupling constants (*J*) are reported in hertz. Mass spectra were recorded on a VG analytical 70-SE spectrometer. Elemental analyses were obtained from Atlantic Microlab Inc. (Norcross, GA) and are within ±0.4 of the theoretical values. The compounds reported as salts frequently analyzed correctly for fractional moles of water. In each case proton NMR showed the presence of water. All chemicals and solvents were purchased from Aldrich Chemical Co., Fisher Scientific, Frontier Scientific, or Lancaster.

**2,5-Bis(3-amidinophenyl)furan Dihydrochloride (DB359).** Divinyl sulfone (5.9 g, 0.05 mol) in 20 mL of dry ethanol was added to a boiling mixture of 3-bromobenzaldehyde (18.5 g, 0.01 mol), anhydrous sodium acetate (2.46 g, 0.03 mol), and 3-benzyl-5-(2-hydroxyethyl)thiazolium chloride (0.27 g, 0.001 mol) in 120 mL of dry ethanol. The mixture was allowed to reflux for 16 h, cooled, filtered, washed with ether and water, and dried. The solid was extracted with boiling chloroform (4 × 200 mL), and the combined chloroform extracts were washed with a 20% $NaHCO_3$ solution and dried over sodium sulfate. The solution was passed through a silica gel column to yield 1,4-bis(3-bromophenyl)butane-1,4-dione as a white crystalline solid (7.90 g, 40%). Mp: 203−204 °C. $^1H$ NMR (DMSO-$d_6$): 8.09 (d, 2H, *J* = 2); 7.89 (t of d, 2H, *J* = 1.6, *J* = 7.6), 7.82 (ddd, 2H, *J* = 0.8, *J* = 2.0, *J* = 8.0), 7.5 (dd, 2H, *J* = 8.0), 3.39 (s, 4H). $^{13}C$ NMR (DMSO-$d_6$): 197.1, 138.4, 135.2, 130.4, 129.9, 126.4, 121.7, 32.3. MS: *m/e* 396 ($M^+$).

To a solution of the above diketone (7.92 g, 0.02 mole) in 80 mL of boiling acetic anhydride were added 5−6 drops of concentrated $H_2SO_4$, and the mixture was heated at reflux for 5 m. The solution was cooled, poured into ice water, and stirred, and the light brown solid which formed was filtered. The solid was washed with water, dissolved in chloroform (200 mL), washed with saturated $NaHCO_3$ and water, and dried over $Na_2SO_4$. The dried solution was passed through a bed of silica gel and after removal of the solvent yielded 5.7 g (75%) of 2,5-bis-(3-bromophenyl)furan as a white crystalline solid. Mp: 130−134 °C. $^1H$ NMR (DMSO-$d_6$): 7.98 (d, 2H, *J* = 1.2), 7.79 (d, 2H, *J* = 8.0), 7.37 (dd, 2H, *J* = 8.0), 7.14 (s, 2H). $^{13}C$ NMR (DMSO-$d_6$): 151.3, 131.8, 130.6, 129.9, 125.7, 122.3, 122.0, 109.3; MS *m/e* 378 ($M^+$)

A mixture of the above dibromofuran (5.0 g, 0.013 mol) and CuCN (4.15 g, 0.046 mol) in 10 mL of dry *N*-methyl-2-pyrrolidone was heated at reflux under $N_2$ for 2 h (monitored by TLC). The mixture was cooled, stirred with 150 mL of 10% aqueous NaCN for 5 h., filtered, and washed with water and dried. The solid was dissolved in warm chloroform and passed through a bed of neutral alumina and after evaporation of the solvent yielded 2,5-bis(3-cyanophenyl)furan as white crystalline needles (2.65 g, 75%). Mp: 230−233 °C. $^1H$ NMR (DMSO-$d_6$): 8.32 (s, 2H), 8.14 (d, 2H, *J* = 8), 7.72 (d, 2H, *J* = 8), 7.63 (dd, 2H, *J* = 8), 7.25 (s, 2H). $^{13}C$ NMR (DMSO-$d_6$): 151.2, 130.7, 130.6, 129.8, 127.7, 126.8, 118.2, 112.1, 109.9. MS *m/e* 270 ($M^+$). Anal. ($C_{18}H_{10}N_2O$) C, H, N.

A mixture of 2.5 g (0.0092 mol) of the above dicyano compound in 35 mL of dry ethanol was saturated while stirring and cooling (0−5 °C) with dry HCl gas. The mixture was stirred at room temperature for 6 days (aliquots of the mixture were monitored by TLC and IR). The mixture was diluted with 75 mL of ether and the resultant solid was filtered, washed with ether, and dried under vacumm at 35 °C to yield 3.72 g (92%) of imidate ester hydrochloride, which was used directly in the next step. A suspension of imidate ester HCl (0.87 g, 0.002 mol) in 30 mL of absolute ethanol was saturated with ammonia at 0−5 °C and the mixture was stirred at room temperature for 12 h. The solvent was removed and the solid was dissolved in ice water, filtered, and basified with cold 2 M NaOH, and the white precipitate which formed was filtered, washed with water, and dried to yield 0.49 g (80%) of free base. The freebase (0.3 g, 0.001mol) was converted into the HCl salt by treating with ethanolic HCl to yield 0.35 g (90%). Mp: 277−279 °C. $^1H$ NMR (DMSO-$d_6$/$D_2O$): 8.18 (brs, 2H), 8.10 (d, 2H, *J* = 7.6), 7.71−7.63 (m, 4H), 7.14 (s, 2H). $^{13}C$ NMR (DMSO-$d_6$): 166.1, 152.5, 131.3, 130.6, 129.3, 129.0, 127.4, 123.3, 110.5. FABMS: *m/e* 305 ($M^+$+1). Anal. ($C_{18}H_{16}N_4O$·2HCl·0.25$H_2O$) C, H, N.

**2,5-Bis[3-(2-imidazolino)phenyl]furan Dihydrochloride (DB361).** A mixture of the above imidate ester HCl (0.87 g, 0.002 mol) and ethylenediamine (0.24 g, 0.004 mol) in 15 mL of dry ethanol was heated under reflux for 12 h. The solvent was removed and the residue was treated with water, filtered, and basified with 5 N NaOH. The precipitated solid was filtered, washed with water, dried, and crystallized from chloroform:ether, to yield an off-white solid (0.57 g, 80%). The free base (0.45 g, 0.0013 mol) was converted into its HCl salt with ethanolic HCl to yield 0.51 g (88%). Mp: 258−261 °C. $^1H$ NMR (DMSO-$d_6$/$D_2O$): 8.65 (s, 2H), 8.16 (d, 2H, *J* = 8), 7.91 (dd, 2H, *J* = 0.8, *J* = 8), 7.67 (dd, 2H, *J* = 8), 7.22 (s, 2H), 4.03 (s, 8H). $^{13}C$ NMR (DMSO-$d_6$): 164.5, 151.9, 130.8, 129.9, 129.4, 127.4, 123.6, 122.8, 110.1, 44.4. FABMS: *m/e* 357 ($M^+$ + 1). Anal. ($C_{22}H_{20}N_4O$·2HCl·$H_2O$) C, H, N.

**2,5-Bis[3-(2-(4,4-dimethyl)imidazolino)phenyl]furan Dihydrochloride (DB471).** A mixture of the above imidate ester HCl (0.87 g, 0.002 mol) and 1,2-diamino-2-methylpropane (0.296 g, 0.004 mol) in 15 mL of dry ethanol was heated at reflux for 12 h. The free base was obtained (0.66 g, 80%), as a white crystalline solid. The free base (0.6 g, 0.0014 mol) was converted, with ethanolic HCl, into the yellow hydrochloride salt (0.68 g, 96%). Mp: 259−262 °C. $^1H$ NMR (DMSO-$d_6$/$D_2O$): 8.97 (s, 2H), 8.22 (d, 2H, *J* = 8.4), 8.08 (d, 2H, *J* = 8.4), 7.70 (dd, 2H, *J* = 8.4), 7.63 (s, 2H), 3.80(s, 4H), 1.53 (s, 12H). $^{13}C$ NMR (DMSO-$d_6$): 161.2, 151.7, 130.5, 129.5, 129.1, 127.3, 123.6, 122.8, 109.8, 61.2, 56.4, 27.0. FABMS: *m/e* 413 ($M^+$ + 1). Anal. ($C_{26}H_{28}N_4O$·2HCl·0.5$H_2O$) C, H, N.

**2,5-Bis[3-(2-imidazolinophenyl)]-3,4-dimethylfuran Dihydrochloride (DB443).** A mixture of 2,5-bis(3-bromophenyl) furan (3 g, 0.0079 mol), paraformaldehyde (4 g), and 80 mL of 48% HBr in acetic acid was stirred for 2 days at room temperature. The mixture was carefully poured into 200 mL of ice water, and the precipitated solid was filtered and washed with water. The solid was dissolved in dichloromethane, washed with 10% $NaHCO_3$ and water, dried over $Na_2SO_4$, and filtered, and the solvent was removed under reduced pressure. The solid was recrystallized from $CHCl_3$:ether (8:2) to yield 2,5-bis(3-bromophenyl)-3,4-dibromomethylfuran as off-white solid (4.3 g, 76%). Mp: 162−163 °C. $^1H$ NMR (DMSO-$d_6$): 7.88 (dd, 2H, *J* = 1.2), 7.68 (dd, 2H, *J* = 1.2, *J* = 8), 7.53 (dd, 2H, *J* = 1.2, *J* = 8), 7.37 (dd, 2H, *J* = 8), 4.64 (s, 4H). $^{13}C$ NMR (DMSO-$d_6$): 150.1, 131.8, 131.2, 130.5, 129.4, 124.9, 123.2, 119.8, 22.6. MS: *m/e* 564 ($M^+$). Anal. ($C_{18}H_{12}Br_4O$) C, H.

A solution of the above dibromomethyl analogue (4 g, 0.0071 mol) in 80 mL of ether:THF (2:1) was added to a well-stirred suspension of LAH (1.3 g, 0.0038 mol) in 30 mL of THF over 10 min. It was stirred at room temperature for 1.5 h, cooled, and carefully decomposed with wet ether, diluted with 200 mL of water, extracted with 2 × 100 mL of $CH_2Cl_2$, and dried over $Na_2SO_4$. The solvent volume was reduced under partial vacuum and the resultant solid was filtered and crystallized from ether:hexane (9:1) to yield 2,5-bis(3-bromophenyl)-3,4-dimethylfuran as a white solid (2.5 g, 87%). Mp: 135−136 °C. $^1H$ NMR (DMSO-$d_6$): 7.69 (d, 2H, *J* = 1.2), 7.67 (d, 2H, *J* = 1.2), 7.41 (dd, 2H, *J* = 8), 7.39 (d, 2H, *J* = 8), 7.24 (dd, 2H, *J* = 8), 2.25 (s, 6H). $^{13}C$ NMR (DMSO-$d_6$): 146.1, 132.5, 130.1,

129.5, 129.3, 128.8, 121.3, 118.6, 113.6, 9.9. MS: *m/e* 406 ($M^+$). Anal. ($C_{18}H_{14}Br_2O$) C, H.

A mixture of the above dibromo analogue (2.03 g, 0.005 mol) and CuCN (1.78 g, 0.2 mol) in 15 mL of *N*-methyl-2-pyrrolidone was heated at reflux under $N_2$ for 1.5 h (TLC monitored), cooled, diluted with water, and stirred with 50 mL of 10% NaCN for 2 h, filtered, washed with water, and dried in air. The light gray solid was chromatographed over neutral alumina using ether, ether:chloroform (1:1) to yield 2,5-bis(3-cyanophenyl)-3,4-dimethylfuran as a white crystalline solid (2.2 g, (74%). Mp: 189−191 °C. $^1$H NMR (DMSO-$d_6$): 8.13 (d, 2H, $J$ = 0.8), 8.03 (dd, 2H, $J$ = 0.8, $J$ = 8), 7.74 (dd, 2H, $J$ = 0.8, $J$ = 8), 7.66 (dd, 2H, $J$ = 8), 2.23 (s, 6H). $^{13}$C NMR (DMSO-$d_6$): 146.1, 132.5, 130.1, 129.5, 129.3, 128.8, 121.3, 118.6, 113.1, 9.1. MS: 298 ($M^+$). Anal. ($C_{20}H_{14}N_2O$). C, H, N.

A mixture of 1.49 g (0.005) of the above dicyano compound in 35 mL dry ethanol was saturated while stirring and cooling (0−5 °C) with dry HCl gas. The mixture was stirred at room temperature for 6 days (aliquots were monitored by TLC and IR). The mixture was diluted with 75 mL of ether, and the resultant solid was filtered, washed with ether, and dried under vacuum at 35°C to yield 1.97 g (85%) of the imidate ester hydrochloride. A mixture of imidate ester HCl (0.92 g, 0.002 mol) and ethylenediamine (0.24 g, 0.004 mol) in 30 mL of dry ethanol was heated at reflux for 12 h, and the solvent was removed under reduced pressure. The resultant solid was treated with water basified with 10% aq NaOH. The precipitated solid was filtered, washed with water, dried, and crystallized with a ethanol:ether mixture to yield 0.64 g (83%) off-white free base. The free base (0.58 g, 0.0015 mol) was converted to its yellow hydrochloride salt with ethanolic HCl (0.63 g, 92%). Mp: 267−269 °C (dec). $^1$H NMR (DMSO-$d_6$/$D_2O$): 8.22 (s, 2H), 8.05 (d, 2H, $J$ = 8), 7.79 (d, 2H, $J$ = 8), 7.7 (dd, 2H, $J$ = 8), 4.0 (s, 4H), 2.22 (s, 6H). $^{13}$C NMR (DMSO-$d_6$/$D_2O$): 165.5, 146.3, 132.2, 131.3, 130.5, 127.2, 125.1, 123.2, 122.1, 44.9, 9.9. FABMS: *m/e* 385 ($M^+$+1). Anal. ($C_{24}H_{24}N_4O$·2HCl) C, H, N.

**2,5-Bis[3-amidinophenyl]thiophene Dihydrochloride (DB495).** To a mixture of 2,5-bis(trimethylstannyl)thiophene (5.11 g, 0.0125 mol) and 3-bromobenzonitrile (4.55 g, 0.025 mol) in 45 mL of dry dioxane was added Pd [($PPh_3$)$_4$] (0.575 g, 2 mol %) under nitrogen. The mixture was heated at reflux for 8 h (TLC monitored), the solvent was distilled under vacuum and the oily residue was dissolved in 200 mL of dichloromethane, and 100 mL of 10% KF (aq) was added. The mixture was stirred for 1 h, filtered through Celite, and washed with water, and the organic layer was dried over $Na_2SO_4$. The solvent was removed under vacuum and the resulting oily residue was chromatographed over silica gel (elution with 3:7 hexane:benzene) to afford 2,5-bis(3-cyanophenyl)-thiophene (2.95 g, 82%) as a white solid. Mp: 178−180 °C. $^1$H NMR (DMSO-$d_6$): 7.87 (dt, 2H, $J$ = 0.8, $J$ = 1.2), 7.82 (ddd, 2H, $J$ = 0.8, $J$ = 1.2 Hz, $J$ = 8), 7.57 (dt, 2H, $J$ = 1.2, $J$ = 8), 7.52 (dt, 2H, $J$ = 0.8, $J$ = 8), 7.35 (s, 2H). $^{13}$C NMR (DMSO-$d_6$): 142.3, 136.1, 131.0, 129.9, 129.7, 129.0, 125.6, 118.3, 113.5. MS: *m/e* 286 ($M^+$). Anal. ($C_{18}H_{11}N_2S$) C, H, N.

The above dicyano compound (2.86 g, 0.01 mol) in 70 mL of ethanol was saturated with dry HCl gas at 0−5 °C and then stirred at room temperature for 7 days (monitored by IR and TLC). Ether was added to the mixture and the yellow imidate ester dihydrochloride was filtered and washed with ether. The solid was dried at 40 °C for 5 h to yield 4.3 g (95%). The hygroscopic solid was used in the next step without further purification. A suspension of imidate ester dihydrochloride (0.9 g, 0.002 mol) in 35 mL of ethanol was saturated with ammonia gas at 0−5°C, stirred at room temperature for 2 days, and the solvent was removed under reduced pressure. The solid was suspended in water, the pH was adjusted to 9, and the pale solid was filtered, washed with water, and dried. The solid was stirred in saturated ethanolic HCl (20 mL) at 50−55 °C for 1 h, treated with ether, filtered, and dried in a vacuum oven at 75 °C for 24 h to yield 0.61 g (77%) of a pale yellow solid. Mp: 305−307 °C (dec). $^1$H NMR (DMSO-$d_6$/$D_2O$): 9.65 (br, 4H), 9.47 (br, 4H), 8.26 (br, 2H), 7.97 (brd, 2H, $J$ = 7.6), 7.85 (brd, 2H, $J$ = 7.6), 7.78 (s, 2H), 7.65 (dd, 2H, $J$ = 7.6). $^{13}$C NMR (DMSO-$d_6$/$D_2O$): 165.3, 141.7, 133.8, 129.9, 129.5, 128.5, 126.8, 126.4, 124.6. FABMS: *m/e* 321 (M + 1). Anal. ($C_{18}H_{16}N_4S$·2HCl·2.25$H_2O$) C, H, N.

**2-(3-Amidinophenyl)-5-(4-amidinophenyl)furan Dihydrochloride (DB555).** To a stirred mixture of 1-(4′-bromophenyl)-3-dimethylaminopropane-1-one hydrochloride (14.0 g, 0.05 mol), 3-benzyl-5-(2-hydroxyethyl)-4-methyl-1,3-thiazolium chloride (0.68 g, 0.0025 mol), and triethylamine (15.15 g, 0.15 mol) in 200 mL of anhydrous dioxane was added 3-bromobenzaldehyde (9.25 g, 0.05 mol), and the mixture was heated at reflux for 12 h (under nitrogen). The solvent was removed and the residue stirred with 200 mL of water, and the gummy mass was extracted with 3 × 20 mL of warm chloroform, washed with 2 × 100 mL of 10% $NaHCO_3$, dried over $Na_2SO_4$, and filtered. After removing the solvent, the residual mass was stirred with 30 mL of ether:ethanol (1:2), and filtration yielded 1-(4-bromophenyl)-4-(3-bromophenyl)butane-1,4-dione as a white crystalline solid (7.96 g, 40%). Mp: 118−119 °C. $^1$ H (NMR (DMSO-$d_6$): 8.10 (dd, 1H, $J$ = 1.6), 8.0 (brd, 1H, $J$ = 7.6), 7.93 (d, 2H, $J$ = 7.6), 7.83 (brd, 1H, $J$ = 7.6), 7.74 (d, 2H, $J$ = 7.6), 7.51 (dd 1H, $J$ = 8), 3.16 (br, 2H), 3.17 (br, 2H). $^{13}$C NMR (DMSO-$d_6$): 197.5, 197.3, 138.5, 135.4, 135.3, 131.5, 130.7, 130.1, 129.6, 126.9, 126.6, 121.8, 32.3, 32.2. MS: *m/e* 396 ($M^+$). Anal. ($C_{16}H_{12}Br_2O_2$) C, H.

A solution of the above diketone (7.92 g, 0.02 mol) in 150 mL of $CHCl_3$:$CH_3OH$ (7:3) was saturated with dry HCl gas at 0−5°C and stirred at 25 °C for 2 h (TLC). The solvent was removed under reduced pressure, the residue was stirred with water, and the solid was filtered, washed with water, suspended in 10% $NaHCO_3$ (150 mL), filtered, washed with water, dried, and recrystallized from $CHCl_3$:ether (3:7) to yield 2-(4-bromophenyl)-5-(3-bromophenyl)furan as a white solid (6.7 g, 89%). Mp: 120−121 °C. $^1$H NMR (DMSO-$d_6$): 7.98 (dd, 1H, $J$ = 1.6), 7.80 (brd, 1H, $J$ = 8), 7.77 (d, 2H, $J$ = 8.8), 7.62 (d, 2H, $J$ = 8.8), 7.48 (brd, 1H, $J$ = 8), 7.39 (t, 1H, $J$ = 8), 7.17 (d, 1H, $J$ = 3.5), 7.11 (d, 1H, $J$ = 3.6). $^{13}$C NMR ($CDCl_3$): 153.0, 152.1, 132.5, 131.9, 130.3, 130.2, 129.4, 126.7, 125.4, 123.0, 122.3, 121.0, 109.4, 107.8. MS: *m/e* 378 ($M^+$). Anal. ($C_{16}H_{10}Br_2O$) C, H.

A mixture of the above dibromo analogue (3.78 g, 0.01 mol) and CuCN (2.67 g, 0.03 mol) in 60 mL of *N*-methyl-2-pyrrolidinone was heated at reflux (under nitrogen) for 2.5 h. The mixture was cooled, diluted with 100 mL water, and stirred with 100 mL of 10% NaCN (aq) for 3 h, filtered, washed with water, and dried. The crude product was dissolved in chloroform and chromatographed over neutral alumina to yield 2-(4-cyanophenyl)-5-(3-cyanophenyl)furan as a pale solid (2.3 g, 85%). Mp: 290−293 °C.

$^1$H NMR (DMSO-$d_6$): 8.30 (t, 1H, $J$ = 1.6), 8.14 (brd, 1H, $J$ = 8), 8.02 (d, 2H, $J$ = 8.5), 7.86 (d, 2H, $J$ = 8.5), 7.74 (brd, 1H, $J$ = 8), 7.65 (m, 1H), 7.32 (d, 1H, $J$ = 4), 7.30 (d, 1H, $J$ = 4). $^{13}$C NMR (DMSO-$d_6$): 151.8, 151.6, 133.4, 132.5, 130.9, 130.5, 128.8, 127.8, 126.9, 123.9, 118.4, 118.0, 112.1, 111.3, 110.2, 109.5. MS: *m/e* 270 ($M^+$). Anal. $C_{18}H_{10}N_2O$) C, H, N.

The above dicyano compound (2.70 g, 0.01 mol) in 60 mL of ethanol was saturated with dry HCl gas at 0−5 °C. The reaction mixture was stirred at room temperature for 7−8 days (monitored by IR and TLC) and diluted with ether, and the yellow imidate ester hydrochloride was filtered, washed with ether, and dried under vacuum for 6 h (3.88 g, 89%). The solid was used in next step without further purification. A suspension of the imidate ester hydrochloride (0.87 g, 0.002 mol), in 25 mL of ethanol, was saturated with ammonia gas at 0−5 °C and stirred for 24 h at room temperature. The solvent was removed under reduced pressure, diluted with water, and basified with 2 N NaOH (aq) to pH 10. The solid was filtered, washed with water, and dried. The solid was dissolved in 15 mL of ethanol, treated with 2 mL of saturated ethanolic HCl, and stirred at 35 °C for 2 h. The solvent was removed under reduced pressure, and the residue was triturated with ether, filtered, washed with ether, and dried under vacuum at 45 °C for 24 h to yield 0.51 g (67%). Mp: 358−360 °C (dec). $^1$H NMR (DMSO-$d_6$/$D_2O$): 8.28 (dd, 1H, $J$ = 1.6 $J$ = 1.2), 8.15

(ddd, 1H, $J = 1.6$, $J = 1.2$, $J = 8$), 8.03 (d, 2H, $J = 8.8$), 7.93 (d, 2H, $J = 8.8$), 7.77 (ddd, 1H, $J = 1.6$, $J = 1.2$, $J = 8$), 7.68, (dd, 1H, $J = 8$), 7.31 (d, 1H, $J = 3.6$), 7.26 (d, 1H, $J = 3.6$). $^{13}$C NMR (DMSO-$d_6$/$D_2O$): 165.4, 165.0, 152.7, 152.0, 134.6, 130.5, 129.9, 128.9, 128.8, 128.6, 127.2, 126.1, 123.9, 123.3, 111.5, 110.3. Anal. ($C_{18}H_{16}N_4O$. 2HCl·0.25$H_2O$). C, H, N.

**2-[4-(*N*-Isopropylamidino)phenyl-5-[3-(*N*-isopropylamidino)phenyl]furan (DB581).** Freshly distilled isopropylamine (0.5 mL, 0.005 mol) was added to the suspension of imidate ester hydrochloride (0.65 g, 0.0015 mol) in 10 mL of dry ethanol, and the mixture was stirred at room temperature for 6 d. The solvent was distilled under vacuum, the residue was treated with ice-cold water, and the pale yellow solution was adjusted to pH 9 with 1 M NaOH. The solid was extracted with $CHCl_3$ and the organic phase was collected and dried over anhydrous $Na_2SO_4$. The solvent was evaporated to dryness and the residue was washed with ether, filtered, dried, and crystallized from $CHCl_3$:ether (1:4) to yield a pale crystalline solid (0.5 g, 90%). Mp: >300 °C. $^1$H NMR (DMSO-$d_6$): 9.31 (br, 4H), 8.22 (s, 1H), 8.13 (d, 1H, $J = 8$), 8.02 (d, 2H, $J = 8$), 7.85 (d, $J = 8$, 2H), 7.64 (m, 2H), 7.35 (d, $J = 3.6$, 1H), 7.31 (d, $J = 3.6$, 1H), 4.12 (m, $J = 6$, 2H), 1.3 (t, $J = 6$, 12H). $^{13}$C NMR (DMSO-$d_6$): 159.0, 157.2, 152.6, 152.2, 138.4, 136.4, 130.5, 129.6, 128.3, 126.8, 125.5, 124.0, 122.7, 121.3, 108.5, 108.3, 43.4, 22.7, 22.6.

The free base (0.4 g, 0.0008 mol) was dissolved in 5 mL of dry ethanol and saturated with dry HCl gas. The resulting mixture was stirred for 15−20 min and the solvent was removed under vacuum. The resulting residue was triturated with dry ether, and the resulting solid was filtered, washed with ether, and dried in vacuo at 60 °C for 24 h to yield yellow crystalline solid (0.45 g, 92%): mp 300 °C. $^1$H NMR (DMSO-$d_6$): 9.75 (d, $J = 8$, 1H), 9.65 (d, $J = 3.6$, 1H), 9.61 (s, 1H), 9.51 (s, 1H), 9.31 (s, 1H), 9.19 (s, 1H), 8.25 (s, 1H), 8.15 (s, 1H), 8.03 (d, $J = 8$, 2H), 7.87 (d, $J = 8$, 2H), 7.67 (m, $J = 8$, 2H), 7.36 (d, $J = 3.6$, 1H), 7.32 (d, $J = 3.6$, 1H), 4.17 (m, $J = 6$, 2H), 1.31 (m, $J = 6$, 12H). Anal. ($C_{24}H_{28}N_40$·2HCl·0.2$H_2O$) C, H, N.

**2-[3-(Amidinopheny)]-5-[4-(amidinopheny)]thiophene Dihydrochloride (DB560).** To a mixture of 2-tributylstannylthiophene (19.6 g, 0.05 mol) and 4-bromobenzonitrile (9.1 g, 0.05 mol) in 45 mL of dry dioxane was added Pd[($PPh_3$)$_4$] (1.15 g, 2 mol %) under nitrogen. The mixture was heated at reflux for 8 h (TLC monitored), the solvent was distilled under vacuum, and the oily residue was treated with 100 mL of dichloromethane and 100 mL of 10% KF (aq). The mixture was stirred for 1 h, filtered through Celite, and washed with water, the organic layer was dried over sodium sulfate, and the solution was concentrated under reduced pressure to yield an oily residue which was chromatographed over silica gel (elution with hexane followed by 3:7 hexane:benzene). 2-(4-Cyanophenyl)thiophene (7.7 g, 83%) was obtained as a white solid. Mp: 85−86 °C. $^1$H NMR (DMSO-$d_6$): 7.81 (brs, 4H), 7.67 (brm, 2H), 7.18 (brm, 1H). $^{13}$C NMR (DMSO-$d_6$): 141.2, 138.0, 132.9, 128.8, 127.9, 126.0, 125.8, 118.6, 109.5. MS: *m/e* 185 ($M^+$).

Bromine (1.76 g, 0.011 mol) in 15 mL of dichloromethane was added over 15 m to a well-stirred solution of 2-(4-cyanophenyl)thiophene (1.85 g, 0.01 mol) in 50 mL of dichloromethane at 5−10 °C. The mixture was stirred at room temperature for 2.5 h. The mixture was diluted with 50 mL of water and 50 mL of dichloromethane. The organic layer was washed with 5% sodium thiosulfate, 5% sodium bicarbonate, and water and dried over sodium sulfate. The solvent was removed under reduced pressure and the residual solid was triturated with ether:hexane (1:4) to yield 2-bromo-5-(4-cyanophenyl)thiophene (2.14 g, 81%) as a off-white crystalline solid. Mp: 98−99 °C. $^1$H NMR (DMSO-$d_6$): 7.83 (d, 2H, $J = 8.4$), 7.78 (d, 2H, $J = 8.4$), 7.53 (d, 1H, $J = 4$), 7.30 (d, 1H, $J = 4$). $^{13}$C NMR (DMSO-$d_6$): 142.7, 136.8, 132.8, 131.9, 126.6, 125.6, 118.3, 112.9, 109.9. MS: *m/e* 264 ($M^+$). Anal. ($C_{11}H_6BrNS$) C, H, N.

Potassium carbonate (3.03 g, 0.022 mol) in 15 mL of water was added to a well-stirred solution of the above 2-(4-cyanophenyl)-5-bromothiophene (2.64 g, 0.01mol) and 3-cyanophenylboronic acid (1.62 g, 0.011 mol) in 30 mL of *n*-propanol, which was followed by addition of tetrakis(triphenylphosphine)palladium (0.23 g, 2 mol %). The reaction mixture was heated at reflux for 12 h (under nitrogen). The solvent was removed under reduced pressure. The residue was diluted with 50 mL of water, filtered, and dried. The solid was dissolved in 100 mL of chloroform and filtered through Celite. The solvent was removed and the solid was crystallized from ether:benzene to yield 2-[3-cyanophenyl]-5-(4-cyanophenyl)-thiophene (2.1 g, 73%) as a bright yellow crystalline solid. Mp: 169−170 °C. $^1$H NMR (DMSO-$d_6$): 8.13 (dd, 1H, $J = 1.6$), 7.96 (ddd, 1H, $J = 0.8$, $J = 1.6$, $J = 8$), 7.83 (brs, 4H) 7.74 (md, 1H, $J = 8$), 7.71 (d, 1H, $J = 4$), 7.62 (d, 1H, $J = 4$), 7.62 (dd, 1H, $J = 8$). $^{13}$C NMR (DMSO-$d_6$): 142.0, 141.5, 137.2, 134.1, 132.7, 131.1, 130.1, 129.6, 128.3, 127.2, 126.7, 125.5, 118.2, 118.0, 112.2, 109.8. MS: *m/e* 286 ($M^+$). Anal. ($C_{18}H_{10}N_2S$) C, H, N.

The above dicyano compound (2.86 g, 0.01mol) in 70 mL of ethanol was saturated with dry HCl gas at 0−5 °C and then stirred at room temperature for 7 days (monitored by IR and TLC). Ether was added to the mixture and the yellow imidate ester dihydrochloride was filtered and washed with ether. The solid was dried at 40 °C for 5 h, to yield 4.3 g (95%). The hygroscopic solid was used in the next step without further purification. A suspension of imidate ester dihydrochloride (0.9 g, 0.002 mol) in 35 mL of ethanol was saturated with ammonia gas at 0−5 °C and stirred at room temperature for 2 days, and the solvent was removed under reduced pressure. The solid was suspended in water, the pH was adjusted to 9, and the pale solid was filtered, washed with water, and dried. The solid was stirred in saturated ethanolic HCl (20 mL) at 50 °C for 1 h, diluted with ether, filtered, and dried in a vacuum oven at 75 °C for 24 h to yield 0.61 g (78%) of a pale yellow solid. Mp: 320−321 °C (dec). $^1$H NMR (DMSO-$d_6$/$D_2O$): 8.12 (dd, 1H, $J = 1.6$, $J = 8$), 8.01 (brd, 1H, $J = 8$), 7.91(d, 2H, $J = 8.8$), 7.88 (d, 2H, $J = 8.8$), 7.76 (d, 1H, $J = 4$), 7.75 (brd, 1H, $J = 8$), 7.72 (d, 1H, $J = 4$), 7.69 (dd, 1H, $J = 8$). $^{13}$C NMR (DMSO-$d_6$/$D_2O$): 165.4, 165.0, 143.0, 141.9, 138.5, 134.2, 130.6, 130.3, 129.3, 128.9, 127.5, 127.0, 126.6, 125.6, 125.0. FABMS: *m/e* 321 ($M^+ + 1$).

**Competition Dialysis.** Competition dialysis experiments were done exactly as previously described.[11−13] The nucleic acids used in the test array are listed in Table 1. The preparation of these nucleic acids is fully described in refs 12 and 13. Competition dialysis studies were done in BPES buffer.

**Thermal Denaturation Studies.** Thermal denaturation studies were done using a Cary 3E spectrophotometer (Varian, Inc., Moutain View, CA) equipped with a Peltier temperature controller.[11] Solutions of poly dA:(poly dT)$_2$ (final concentration of 20 $\mu$M expressed in triplets) in BPES buffer were prepared by direct mixing with aliquots from ligand stock solution, followed by incubation for 12 h at 24 °C to ensure equilibration. Samples were heated at a rate of 1 °C min$^{-1}$ while continuously monitoring absorbance at 260 nm.

**Computational Methods.** The three different planar low-energy conformations of DB359 were obtained by rotating the phenyl furan bond, and each conformation was docked into a central intercalation site of the triplex $dT_6$·$dA_6$·$dT_6$ followed by energy minimization. The coordinates of the triplex and central intercalation site used in this study were generated as previously described for the $dT_{10}$·$dA_{10}$·$dT_{10}$ triplex 10mer.[19,20]

Each minimized complex was then immersed in a periodic box of TIP3P[21] water molecules. Fifteen $Na^+$ ions were place around the complex using the Leap module in AMBER to obtain electrostatic neutrality. The atomic charges and force field parameters of DB359 were determined using the RESP[22] methodology at the HF/6-31G* level of theory in Gaussian 98 and comparable parameters of the Cornell et al. force field.[23] All minimization and molecular dynamics simulations were carried out using the Amber 5[24] suites of program. The complexes were equilibrated by using a multistage equilibration protocol previously described.[25,26] After equilibration, each final structure was subjected to 1 ns of molecular dynamics simulation in the isobaric−isothermal ensemble at a constant

**Table 1.** Nucleic Acid Samples Used in Competition Dialysis Experiments

| conformation | nucleic acid | $\lambda$ (nm) | $\epsilon$ ($M^{-1}$ $cm^{-1}$) | monomeric unit |
|---|---|---|---|---|
| single-strand pyrimidine | poly dT | 264 | 8 520 | nucleotide |
| single-strand purine | poly dA | 257 | 8 600 | nucleotide |
| duplex DNA | *C. perfringens* (31% GC) | 260 | 12 476 | base pair |
| | calf thymus (42% GC) | 260 | 12 824 | base pair |
| | *M. lysodeikticus* (72% GC) | 260 | 13 846 | base pair |
| | poly dA:poly dT | 260 | 12 000 | base pair |
| | $[poly\ (dAdT)]_2$ | 262 | 13 200 | base pair |
| | $[poly\ (dGdC)]_2$ | 254 | 16 800 | base pair |
| duplex RNA | poly rA:poly rU | 260 | 14 280 | base pair |
| DNA:RNA hybrid | poly rA:poly dT | 260 | 12 460 | base pair |
| Z DNA | $[Br\text{-}poly\ (dGdC)]_2$ | 254 | 16 060 | base pair |
| triplex DNA | poly dA:$(poly\ dT)_2$ | 260 | 17 200 | triplet |
| quadruplex DNA | $(5'T_2G_{20}T_2)_4$ | 260 | 39 267 | tetrad |

[a] Key: $\lambda$, wavelength; $\epsilon$, molar extinction coefficient at the wavelength $\lambda$, expressed in terms of the monomeric unit specified.

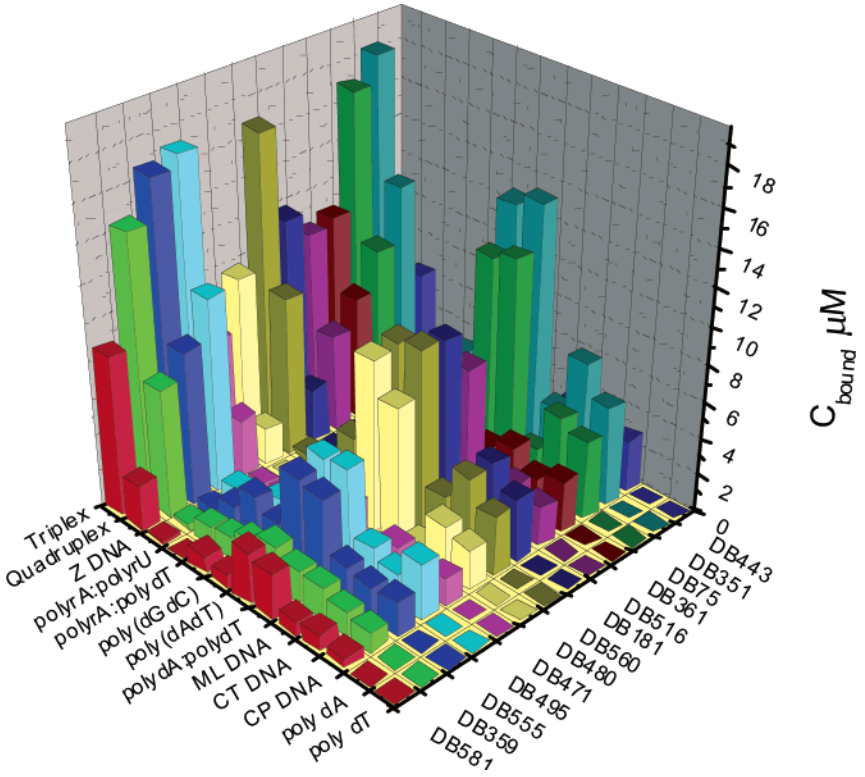


**Figure 2.** Comparative binding of 13 aromatic diamidine derivatives to 13 nucleic acid structures.

temperature of 300 K and pressure of 1 bar. The SHAKE[27] algorithm was applied to all bonds involving a hydrogen atom, thus allowing a time step of 2.0 fs in solving the Newton's equations of motion. The particle mesh Ewald[28] method was used to treat the long-range electrostatic interactions, and the nonbonded van der Waals interactions were subjected to a 9 Å cutoff. Structures were collected at time steps of 1ps. The last 100 ps of each simulation (100 structures) was averaged and the average structure was energy minimized. The interaction energy of each complex was calculated from the average structures by subtracting the energies of the free triplex and the free drug from that of the complex.

## Results

Figure 2 shows the results of competition dialysis experiments using the aromatic diamidines shown in Figure 1. The interaction of 13 compounds with 13 different nucleic acid structures and sequences (Table 1) was studied. Several generalities may be seen at a glance in Figure 2. None of the compounds bind to single-stranded DNA as represented by poly dA and poly dT. In contrast, all compounds bind tightly to the DNA triplex poly dA:$(poly\ dT)_2$, often better than to duplex DNA forms. All compounds also bind well to the parallel stranded qudruplex $(T_2G_{20}T_2)_4$, but not as well as to the triplex. There is little or no interaction with duplex RNA, with a DNA:RNA hybrid, or with left-handed Z DNA. Compound binding to duplex DNA forms is highly variable and depends on base composition and sequence.

Figure 3 shows the contrasting binding pattern of the aromatic diamidines to those of common intercalating and groove-binding compounds. Data are presented as Tukey box plots,[29] a graphical tool that concisely summarizes the properties of distributions. In a box plot, the horizontal line within the box marks the 50th percentile, while the square symbol marks the arithmetic mean. The top edge of the box marks the 75th percentile and the lower edge the 25th percentile. The verticle lines extending from the box mark the 90th (top) and 10th (bottom) percentiles. Crosses mark the 1st and 99th percentiles, and bars mark the complete range of the data. The plots in Figure 3 show the distribution of binding to each of the 13 nucleic acid structures

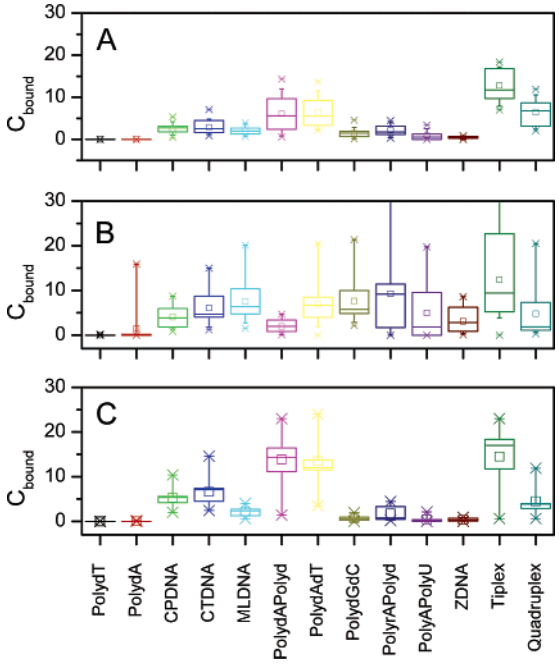


**Figure 3.** Comparison of the binding of aromatic diamidines (A) to that of standard intercalators (B) and groove binders (C). Data are presented as Tukey box plots, a graphical tool that concisely summarizes the properties of distributions as described in the text. The standard intercalators represented in panel B include actinomycin D, ethdium bromide, propidium iodide, 9-aminoacridine, quinacrine, daunorubicin, doxorubicin, coralyne, thiazole orange, and ellipticine. The groove binders represented in panel C include berenil, distamycin, DAPI, DB75, DB351, DB181, and methyl green.

observed in competition dialysis experiments for each class of compound.

The binding pattern for the aromatic diamidines (Figure 3A) is clearly distinct from those observed for common intercalators (Figure 3B) and groove binders (Figure 3C). The aromatic diamidines show significant binding to only AT-containing DNA duplexes, to the TAT triplex, and to the parallel quadruplex structure. Intercalators, as a class, show far less binding specificity and bind to most structures in the assay, except for single-stranded DNA and poly dA:poly dT. Intercalators show a general preference for GC-rich duplex DNA, and bind strongly to duplex RNA and to a DNA:RNA hybrid structure. Groove binders strongly prefer binding to poly dA:poly dT and [poly (dAdT)]$_2$ over all other single- and double-stranded structures. While groove-binders appear to bind strongly to triplex DNA, such binding is illusory and was previously shown to arise from displacement of the third strand and tight binding to the resultant duplex.[11] The most noticeable differences between groove-binders and the aromatic diamidines are the greater binding of the latter to the parallel-stranded G-quadruplex structure, along with lesser binding to the AT-rich natural DNAs.

Competition dialysis results for two compounds, DB75 and DB359, are shown in Figure 4 to facilitate detailed comparison. DB75 is the parent compound of the aromatic diamidines, while DB359 is a positional isomer in which the amidine substituents were shifted from the para−para orientation to the meta−meta orientation. The change in geometry dramatically alters the structural preferences for binding. Both DB75 and DB359 bind strongly to triplex and quadruplex structures. Binding to duplex forms, however, is greatly diminished for DB359 relative to DB75. The result is to render DB359 more structurally selective than DB75, not by enhancing triplex affinity but rather by reducing affinity toward all other structural forms.

The structural selectivity of the aromatic diamidines can be quantitatively compared by use of the *specificity sum*, SS.[30] To compute the specificity sum, binding profiles such as shown in Figure 4 are first normalized with respect to the maximal amount bound ($C_{max}$) to any of the structures. The normalized amounts bound are then simply summed. The specificity sum is thus defined as

$$SS = \sum_{i=1}^{13} \frac{C_{b,i}}{C_{max}}$$

Since thirteen structures are used in this version of the competitions dialysis assay, SS ranges from 1 (binding to only one structure; maximal structural selectivity) to 13 (equal binding to all structures; no structural selectivity). The data shown in Figure 4 yield SS = 4.0 for DB75 and SS = 2.3 for DB359. Values for the specificity sum for all compounds studied are shown in Figure 5A and in Table 2. SS ranges from 2.3 to 4.9 for the various aromatic diamidines. In a study of 126 compounds from a wide variety of chemical classes, an average value of SS = 4.5 ± 2.0 was found (J. B. Chaires, unpublished data). The aromatic diamidines studied here are thus all more structurally selective than average, in particular because of their general preference for the triplex structure. (On the basis of the average of multiple experiments, we estimate that the amount of ligand bound to each nucleic acid structure is determined with 5−10% error. Since SS is a sum of normalized values, its error would be roughly equal to the largest numerical error among the quantities summed, based on the rules of error propagation. We therefore believe that SS values are accurate to approximately 10%.)

While the metric SS is a measure of structural selectivity, it does not contain information about compound affinity. A compound might bind selectively to a particular structure, but it may bind weakly. The ratio $C_{max}$/SS is therefore of interest, since it provides a measure of both selectivity and affinity.[30] $C_{max}$ is the maximal amount of ligand bound to any structure and is directly proportional to binding affinity. If $C_{max}$ is large (high affinity) and SS is small (high selectivity), the largest value for the ratio $C_{max}$/SS will result. In the study of 126 compounds, a range in $C_{max}$/SS values of 0.06 to 9.8 was found, with an average of $C_{max}$/SS = 2.4 ± 2.2. Values for $C_{max}$/SS for the aromatic diamidines are shown in Figure 5B and Table 2. Values range from 1.6 to 6.2, indicating that the aromatic diamidines possess greater combined affinity and selectivity than average.

Comparison of SS and $C_{max}$/SS values identifies compounds with the greatest combined selectivity and affinity. In Figure 5A, for example, DB581 and DB359 show equal specificity sums and are the most selective compounds of the group. However, inspection of Figure 5B shows that DB359 binds with higher affinity than

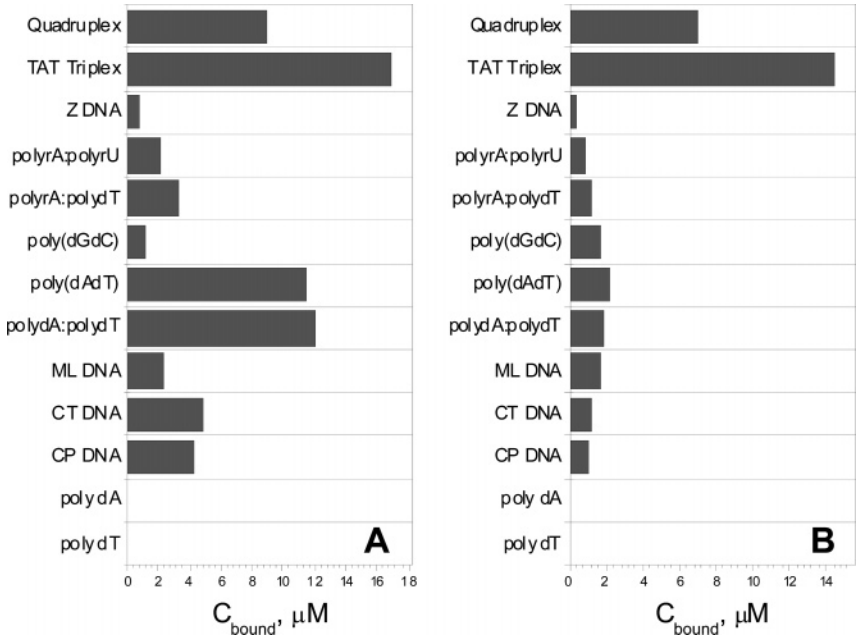


**Figure 4.** Results of competition dialysis experiments using DB75 (A) and DB359 (B).

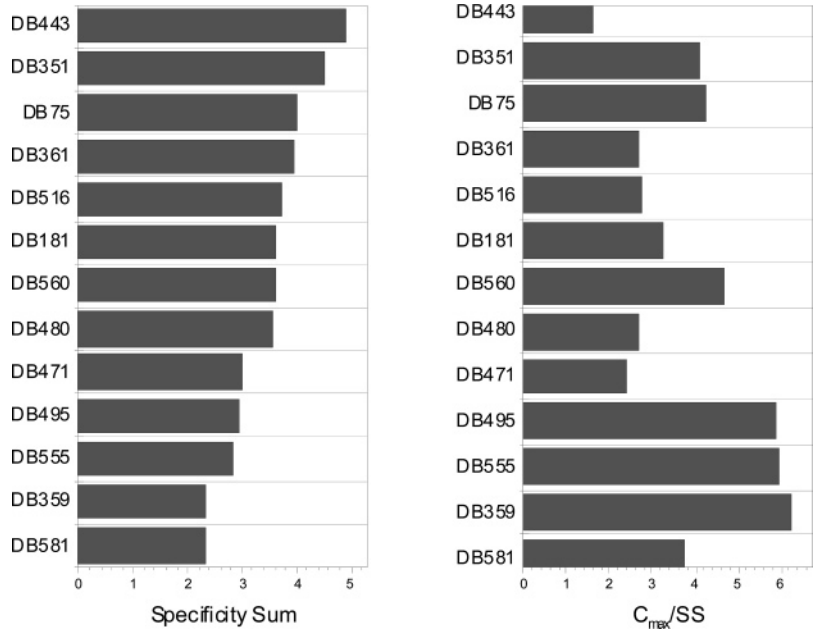


**Figure 5.** Values of the specificity sum, SS, and the ratio $C_{max}$/SS (in $\mu$M) for aromatic diamidine compounds.

does DB581, as reflected by a larger $C_{max}$/SS ratio. On the basis of SS and $C_{max}$/SS values, DB359, DB555, DB495, and DB560 are identified as the four compounds with the most improved combined selectivity and affinity relative to the parent compound DB75. All four compounds show clear selectivity for triplex DNA and to a lesser extent for the parallel quadruplex structure. All strongly prefer multistranded structures over any duplex or single-stranded form in the assay. These four compounds are all either meta−meta or meta−para isomers of DB75 and DB351, and it is clear that the para to meta isomerization causes a significant enhancement of triplex binding specificity.

Competition dialysis data may be used to calculate apparent free energies for binding interactions of any of the structures in the assay.[12] The apparent binding constant for any structure is given by

$$K_{app} = \frac{C_b}{C_f(C_T - C_b)}$$

where $C_b$ is the amount bound (as shown in the examples in Figures 2 and 4), $C_f$ is the free ligand concentration (maintained at 1 $\mu$M in the assay protocol), and $C_T$ is the total nucleic acid concentration (fixed at 75 $\mu$M in the assay protocol). Binding free energies may then be calculated by the standard relation

$$\Delta G_{app} = -RT \ln K_{app}$$

where $R$ is the gas constant and $T$ the temperature in degrees kelvin. Values of $\Delta G_{app}$ for selected structures are listed in Table 2. (Binding constants obtained by competition dialysis have been validated in many cases by studies in which more laborious spectrophotometric

**Table 2.** Selected Binding Properties of Aromatic Diamidines

| compd | SS | $C_{max}$/SS, $\mu$M | $\Delta G_{CT\ DNA}$, kcal mol$^{-1}$ | $\Delta G_{poly\ (dAdT)}$, kcal mol$^{-1}$ | $\Delta G_{Triplex}$, kcal mol$^{-1}$ | $\Delta G_{Quadruplex}$, kcal mol$^{-1}$ |
|---|---|---|---|---|---|---|
| DB581 | 2.32 | 3.74 | −5.55 | −6.22 | −6.96 | −6.15 |
| DB359 | 2.32 | 6.23 | −5.74 | −6.11 | −7.31 | −6.81 |
| DB555 | 2.81 | 5.94 | −5.95 | −6.62 | −7.42 | −6.92 |
| DB495 | 2.92 | 5.88 | −5.91 | −6.67 | −7.44 | −7.09 |
| DB471 | 2.98 | 2.36 | −5.73 | −6.07 | −6.82 | −6.32 |
| DB480 | 3.57 | 2.71 | −6.21 | −7.00 | −7.03 | −6.05 |
| DB560 | 3.60 | 4.67 | −6.53 | −7.02 | −7.42 | −6.96 |
| DB181 | 3.64 | 3.23 | −6.53 | −6.94 | −7.16 | −6.26 |
| DB516 | 3.71 | 2.78 | −6.18 | −6.86 | −7.07 | −6.63 |
| DB361 | 3.98 | 2.68 | −6.10 | −6.37 | −7.09 | −6.79 |
| DB075 | 4.01 | 4.23 | −6.57 | −7.15 | −7.43 | −6.97 |
| DB351 | 4.50 | 4.08 | −6.82 | −7.27 | −7.49 | −7.17 |
| DB443 | 4.90 | 1.62 | −6.23 | −6.34 | −6.89 | −6.75 |

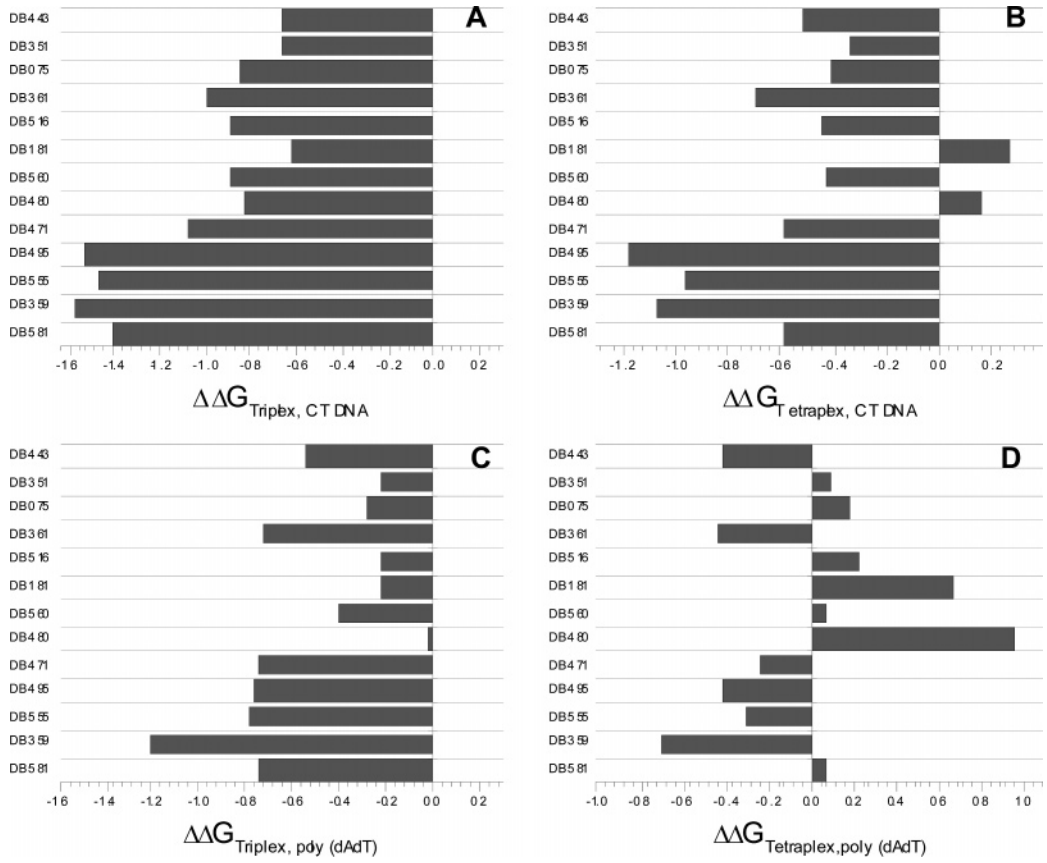


**Figure 6.** Free energy difference plots (kcal mol$^{-1}$) for the binding of aromatic diamidines to triplex (A, C) and quadruplex (B, C) DNA. For panels A and B, duplex calf thymus DNA was taken as the reference. For panels C and D, duplex [poly (dAdT)]$_2$ was taken as the reference. Negative values indicate tighter binding to the triplex or quadruplex stuctures relative to the duplex forms. Positive values indicate weaker binding.

titrations were done to obtain binding constants. Figure S1 in Supporting Information shows the validation).

Selected free energy difference plots are shown in Figure 6. Differences in apparent binding free energies between multistranded triplex and quadruplex forms and reference duplex structures are shown for all aromatic diamidines. Calf thymus DNA and duplex poly (dAdT) were used as reference duplexes. The notation "$\Delta\Delta G_{Triplex,CT\ DNA}$", as an example, signifies the difference in binding free energies between triplex DNA and calf thymus DNA, using the values listed in Table 2. In these difference plots, negative values indicate more favorable binding to the multistranded form relative to the duplex form, while positive values indicate less favorable interactions. Figure 6A,C shows that most aromatic diamidines prefer the triplex poly dA:(poly dT)$_2$ over both calf thymus DNA and duplex poly (dAdT). The only exception is DB480, which binds about equally well to the triplex and to poly (dAdT). Figure 6B,D shows that the differential binding to the parallel stranded quadruplex $[T_2G_{20}T_2]_4$ is more variable than to triplex DNA. All compounds except DB181 and DB480 prefer the quadruplex over calf thymus DNA. The relative aversion of these two compounds for the quadruplex structure is even greater when poly (dAdT) is taken as the reference duplex.

From the data shown in Figures 5 and 6 and Table 2, three compounds stand out as having improved structural selectivity than the parent compound DB75. These compounds are DB359, DB495, and DB555. For these compounds, binding to the triplex poly dA:(poly dT)$_2$ is greatly enhanced relative to any duplex form. To

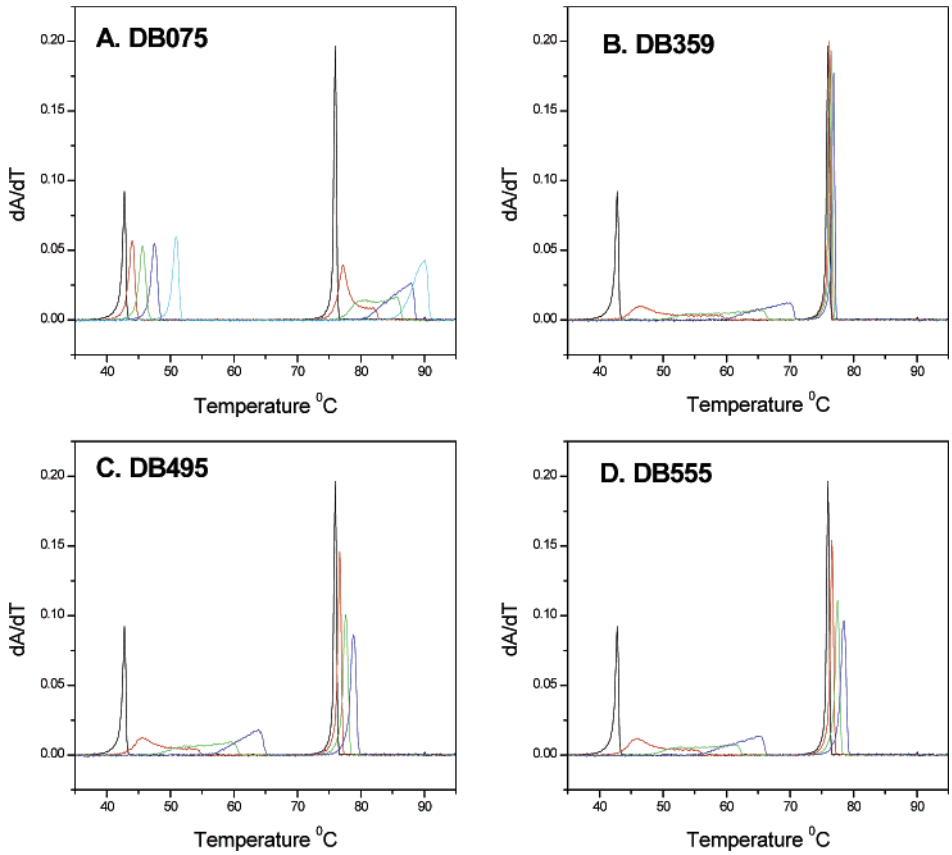


**Figure 7.** Thermal denaturation studies of selected aromatic diamidines. Differential melting curves for the denaturation of the poly dA:(poly dT)$_2$ triple helix is shown as a function of added DB75 (A), DB359 (B), DB495 (C), and DB55 (D). The molar ratios (mol compound/mol triplet) of added compounds are indicated in Figure 8. Under the ionic conditions of these experiments, in the absence of added ligand, the melting of the triplex occurs at 42.8 °C and melting of the duplex occurs at 76.0 °C.

confirm the preference for triplex, thermal denaturation studies were done as shown in Figure 7. Differential melting curves are shown in Figure 7. In the absence of added ligand, the third strand dissociates at $T_m \approx$ 43 °C, while the remaining duplex melts at $T_m \approx 76$ °C. Figure 7A shows that DB75 stabilizes both triplex and duplex forms. The change in $T_m$ as a function of the molar ratio of added DB75 is shown in Figure 8A. DB75 clearly stabilizes the duplex to a greater extent than it does the triplex form, an observation consistent with the competition dialysis data shown in Figure 4A. In contrast, as shown in Figures 7B and 8B, DB359 almost exclusively stabilizes the triplex form and has little affect on duplex melting. That observation is fully consistent with the competition dialysis data shown in Figure 4B. DB495 and DB555 (Figures 7C,D and 8C,D) show behavior that is between that seen for DB75 and DB359. DB495 and DB555 dramatically stabilize the triplex form, but they also stabilize the duplex, although to a far lesser extent than observed for DB75.

To construct plausible molecular models for the DB359−DNA complexes to help understand the strong and preferential binding of DB359 to triplex DNA, several molecular mechanics simulations were conducted with DB359 docked into duplex and triplex DNA (Figure 9), and these were compared to results for DB75. Crystal structures are available from the Neidle laboratory for complexes of DB75 and several derivatives with an AATT minor groove binding site.[3,8,31] In the complexes the furan oxygen points into the minor groove, edges of the two phenyls make close contact with the edges of AT base pairs at the floor of the groove, and the amidines form H-bonds with C2 keto groups of T bases that project into the groove. The entire molecular system makes excellent contacts with the walls of the minor groove to create a complex that is well-optimized for the structure of the para−para aromatic system and the AT minor groove. An obvious initial difference between DB75 and DB359 can be seen in Figure 9. While rotation about the phenyl−amidine or phenyl−furan bonds in DB75 does not change the molecular conformation, similar rotations in DB359 do produce different conformations.[14] Two conformations of DB359 have the amidines pointed in the same direction, either away from the furan O (linear form, upper left in Figure 9) or in the same direction as the O (curved form, lower right in Figure 9). In the linear form, only one amidine at a time can H-bond with AT bases at the floor of the groove, because of steric hindrance from the hydrogen atoms of the furan that also point into the groove. This conformation does not have sufficient curvature to match the DNA minor groove shape. In the curved form, the amidines are very close, and although both could form H-bonds, this complex is destabilized by charge repulsion, and the entire phenylfuran aromatic system is pushed out of the groove, so there is little favorable contact with the bases and walls of the groove. This conformation is too highly curved to match the groove shape. Neither of these complexes nor any with the amidines pointed in opposite directions are as favorable as that for DB75, and as can be seen in Figure 4, DB359

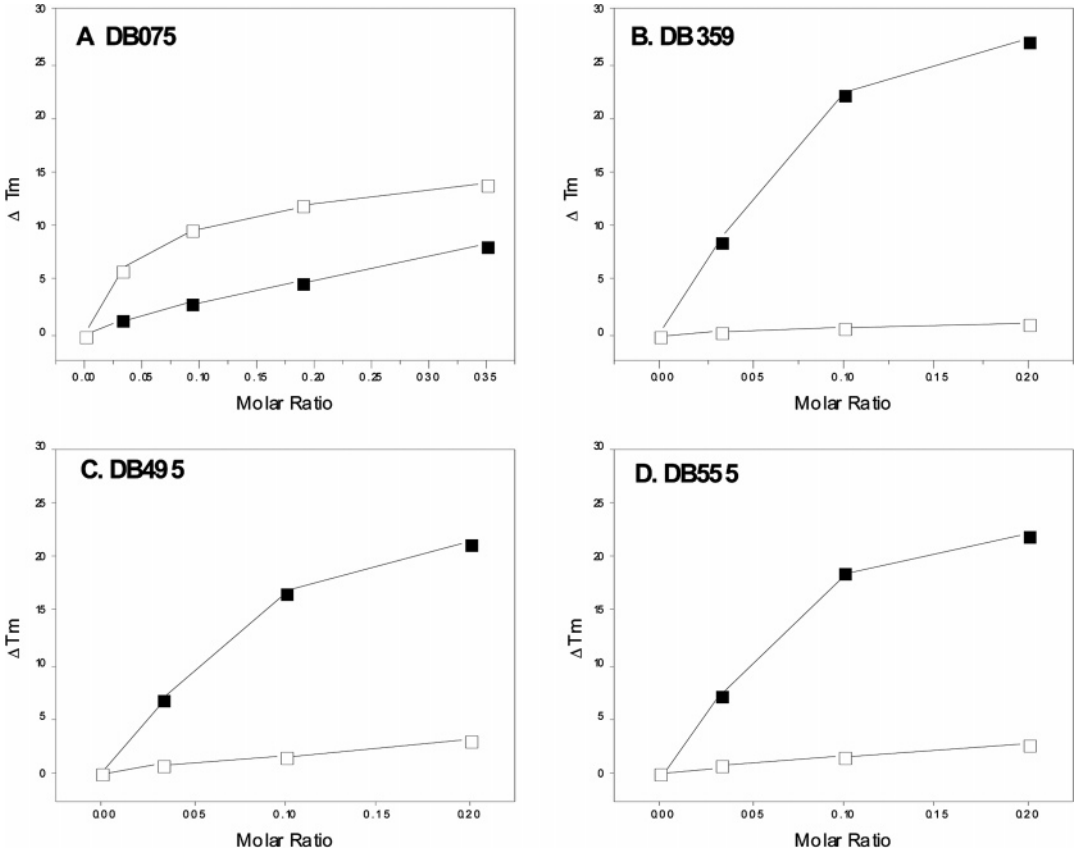


**Figure 8.** Change in the melting temperature ($\Delta T_m$) in response to the addition of cationic furans. The change in the triplex $T_m$ is shown by solid squares, while the change in duplex $T_m$ is shown by open squares. Data are shown for DB75 (A), DB359 (B), DB495 (C), and DB555 (D). For multiphasic melting profiles, the $T_m$ was defined as the temperature at the half-maximal absorbance change.

binds more weakly to all AT-containing DNA duplexes than DB75.

As can also be seen in Figure 4, the situation with triplex binding is quite different, with both compounds forming very favorable complexes. In docking experiments with the triplex, no low-energy groove model could be found with these compounds. Low-energy triplex intercalated complexes are possible with both DB359 and DB75, in agreement with experimental results, and models with DB359 are shown as examples in Figure 9. The lowest energy complex is formed with the linear conformation (upper left in the Figure), and it has excellent overlap of the DB359 aromatic system with the TAT base triplet, one amidine in the minor groove, and one amidine in the groove formed by the A strand and the Hoogsteen T strand. The other groove, formed by the two T strands, contains both T-$CH_3$ groups and is more sterically constrained, more nonpolar than the other two grooves, and is a less favorable amidine docking site. Optimized complexes of other conformations of DB359 have less favorable aromatic overlap and/or less favorable amidine interactions to give higher complex interaction energies. The curved conformation of DB359 (lower right in Figure 9), for example, has the optimum complex conformation with the amidines in the same groove as with the linear complex, but both the aromatic overlap and the amidine interactions are less favorable than with the linear complex. All other complexes have even less favorable interactions energies. An intercalated complex of DB75 that is very similar to that in the upper left of Figure 9 can be formed. The DB75 complex has the furan O pointed in the opposite direction to the DB359 complex, and the curvature of the molecular system places the amidines in the same grooves as in the DB359 complex.

## Discussion

The competition dialysis studies described here show that the aromatic diamidines display a unique pattern of structural selectivity, a pattern that is distinct from the patterns of classic intercalators or groove-binding agents. Aromatic diamidines, in general, bind preferentially to the triplex poly dA:(poly $dT)_2$. Certain compounds, such as DB359, exhibit a particularly high selectivity for the triplex, derived not from greater affinity for the triplex, but rather from reduced binding affinity for all other structures. We note that the poly dA:(poly $dT)_2$ triplex is but one possible triple-helix form. How the aromatic diamidines interact with triple helices with different sequences and strand orientation requires further study and would require competition dialysis experiments using a more extensive array of triplex structures.

DB359 is, in fact, one of the most triplex selective compounds discovered to date. Table 3 compares the selectivity and affinity of several compounds. The structures of these compounds are shown in the Supporting Information (Figure S2). The pronounced triplex selectivity of naphthylquinolines, exemplified by MHQ12, was recently described in detail.[30] MHQ12 emerged from a rational design effort aimed at targeting triplex

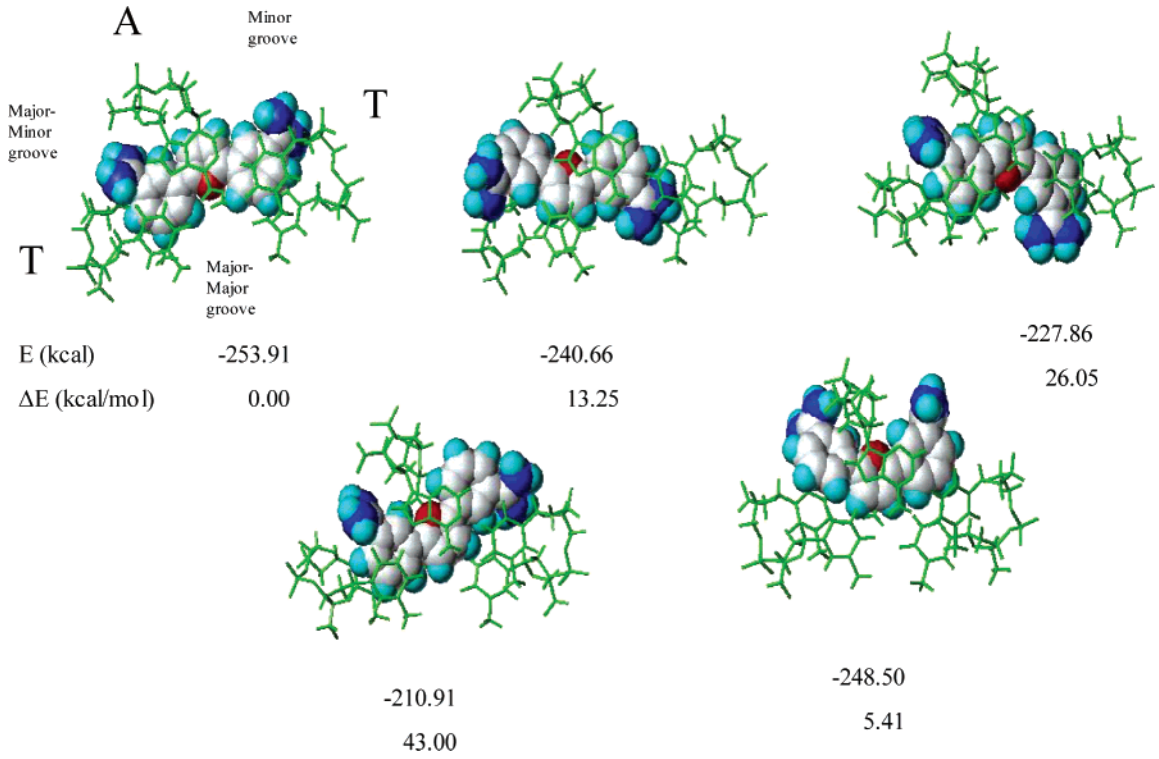


**Figure 9.** The five lowest energy molecular models for the interaction of DB359 with triplex DNA are shown. Molecular mechanics energies ($E$) are shown below the models, and for comparison, $\Delta E$ values relative to the lowest energy structure in the upper left are included. DB359 is shown in space-filling representation (carbon, white; hydrogen, light blue; nitrogen, dark blue; oxygen, red) and the base triplets above and below the intercalated compound are shown as green tubes. Different conformations of DB359, created by rotation about the phenyl−furan bonds, were docked into different orientations of a triplex intercalation site and energy minimized as described in the text.

**Table 3.** Properties of Triplex-Binding Compounds

| compound | SS | $C_{max}$/SS | $\Delta G_{Duplex}$ | $\Delta G_{Triplex}$ |
|---|---|---|---|---|
| MHQ12[30] | 1.32 | 8.93 | −4.2 | −7.0 |
| α-Naphthoflavone[33] | 1.43 | 3.67 | 0 | −6.5 |
| berberine[11] | 1.59 | 3.55 | −4.7 | −6.6 |
| DB359 | 2.34 | 6.23 | −5.7 | −6.95 |
| coralyne[11] | 4.34 | 5.22 | −6.3 | −7.5 |
| DB75 | 4.01 | 4.23 | −6.6 | −7.4 |
| ethidium[11] | 5.05 | 1.93 | −6.4 | −6.5 |
| 2,6-anthraquinone[34] | 5.08 | 2.55 | −6.1 | −6.7 |
| BePI[35] | 6.39 | 1.38 | −6.5 | −6.8 |

structures and is by all measures the most selective triplex binder designed and synthesized so far.

The selectivity and triplex affinity of DB359 compare favorably to those of MHQ12, although its interactions with triplex are serendipitous and were not achieved by design. Several interesting points of comparison emerge from the data of Table 3. Berberine and α-naphthoflavone, for example, are both more selective than DB359, as judged by the SS parameter. Neither compound, however, binds as tightly as does DB359 and consequently have lower $C_{max}$/SS values. Coralyne and DB75 show the highest triplex binding affinity of the compounds listed in Table 3, but their selectivity is compromised by significant binding to other structures and sequences. Optimizing selectivity for a particular target is thus not simply a matter of maximizing its affinity for that target but also of reducing compound affinity for competing structures.

The enhanced triplex selectivity of DB359 relative to the parent compound DB75 results from a geometry change in which the amidine substiuents are shifted from the para−para orientation to the meta−meta orientation. Molecular modeling studies (Figure 9) provide a rationale for the enhanced selectivity. The energetically most favorable structure of the DB359−triplex complex (Figure 9A) is one in which the compound rings are optimally stacked over the base triplets, with the amidines oriented to occupy the minor and major−minor grooves of the TAT triplex. Placing the amidines in the para−para orientations, as in DB75, also allows favorable stacking over the base triplets and proper positioning of the amidines in the triplex grooves. DB75, however, also has a very favorable conformation for interaction with the minor groove in duplex sequences of four or more AT base pairs. We cannot rule out the possibility at this time that DB75 also binds to the triplex grooves. It can clearly intercalate well with the triplex, and for the usual wide minor groove of the triplex, groove binding may be less favorable. Our previous study of naphthylquinolines revealed the vital importance of substituent groove binding to triplex binding affinity.[30] A QSAR was built that correlated the triplex binding affinity of a series of naphthylquniolines with the solvent accessible surface area of substituents that would occupy triplex grooves. The model for the DB359−triplex complex reinforces the importance of groove interactions as a determinant of triplex selectivity and affinity.

The vital role of geometry as a determinant of selectivity for triplex is reinforced by the data obtained for the compounds DB351 and DB495. For these compounds, the furan core was replaced by a thiophene. In DB351, the amidines are in the para−para orientation, while in DB495 the orientation is shifted to meta−meta.

The geometry change renders DB495 more selective than DB351 (Figure 5). These compounds reveal an additional effect. Substitution of sulfur for oxygen (in the change of the furan to the thiophene) slightly reduces selectivity. Thus, the SS value of DB351 is larger than that for DB75, and the SS value of DB495 is greater than that for DB359. The reason for this behavior is not entirely clear, but may result simply from the larger radius of sulfur relative to oxygen, which could perturb stacking interactions within the binding site.

Compounds DB555 and DB560 are para−meta isomers of the parent compounds DB75 and DB351, respectively**.** The para−meta isomers are both more selective than the parents. Interestingly, the difference in selectivity between DB555 and DB560 is more pronounced than observed between DB359 and DB495. The effect of changing the furan to thiophene thus seems to be more pronounced for the para−meta isomers than for the para−para isomers.

The possible biological consequence of triplex binding by the aromatic diamidines is unknown. Tracts containing runs of poly purines/poly pyrimidines can, under superhelical stress, form intramolecular triple helix structures, so-called "H-DNA".[32] The biological role of H-DNA has not been definitively established, but the nonrandom distribution of sequences that can form the structure within genomes suggests that it may play a role in the regulation of gene expression. If so, selective binding to H-DNA by the aromatic diamidines may contribute to their clinical mode of action. Alternatively, triplex binding would represent a significant competitive binding reaction that could effectively reduce compound binding to its preferred duplex target.

**Acknowledgment.** Support was provided by grant CA35635 from the National Cancer Institute (J.B.C.) and grant GM61587 from the National Institute of General Medicine (W.D.W. and D.W.B.). J.B.C. holds the James Graham Brown Endowed Chair in Biophysics, and he thanks the James Graham Brown Foundation for its support.

**Supporting Information Available:** Figures showing the validation of binding constants obtained by competition dialysis and structures of the compounds listed in Table 3 and a table of analysis data for the compounds produced. This material is available free of charge via the Internet at http://pubs.acs.org.

## References

(1) Wemmer, D. E. Designed sequence-specific minor groove ligands. *Annu. Rev. Biophys. Biomol. Struct.* **2000**, *29*, 439−461.
(2) Wemmer, D. E. Ligands recognizing the minor groove of DNA: Development and applications. *Biopolymers* **1999**, *52*, 197−211.
(3) Neidle, S. DNA minor-groove recognition by small molecules. *Nat. Prod. Rep.* **2001**, *18*, 291−309.
(4) Bailly, C.; Chaires, J. B. Sequence-specific DNA minor groove binders. Design and synthesis of netropsin and distamycin analogues. *Bioconjugate Chem.* **1998**, *9*, 513−538.
(5) Tidwell, R. R.; Boykin, D. W. Dicationic DNA Minor Groove Binders as Antimicrobial Agents. *Small Molecule DNA and RNA Binders: From Synthesis to Nucleic Acid Complexes*; Wiley-VCH: New York, 2003; pp 416−460.
(6) Lansiaux, A.; Tanious, F.; Mishal, Z.; Dassonneville, L.; Kumar, A.; et al. Distribution of furamidine analogues in tumor cells: Targeting of the nucleus or mitochondria depending on the amidine substitution. *Cancer Res.* **2002**, *62*, 7219−7229.
(7) Neidle, S.; Nunn, C. M. Crystal structures of nucleic acids and their drug complexes. *Nat. Prod. Rep.* **1998**, *15*, 1−15.
(8) Laughton, C. A.; Tanious, F.; Nunn, C. M.; Boykin, D. W.; Wilson, W. D.; et al. A crystallographic and spectroscopic study of the complex between d(CGCGAATTCGCG)2 and 2,5-bis(4-guanylphenyl)furan, an analogue of berenil. Structural origins of enhanced DNA-binding affinity. *Biochemistry* **1996**, *35*, 5655−5661.
(9) Wilson, W. D.; Tanious, F. A.; Ding, D.; Kumar, A.; Boykin, D. W.; et al. Nucleic Acid Interactions of Unfused Aromatic Cations: Evaluation of Proposed Minor-Groove, Major-Groove and Intercalation Binding Modes. *J. Am. Chem. Soc.* **1998**, *120*, 10310-.
(10) Mazur, S.; Tanious, F. A.; Ding, D.; Kumar, A.; Boykin, D. W.; et al. A Thermodynamic and Structural Analysis of DNA Minor-groove Complex Formation. *J. Mol. Biol.* **2000**, *300*, 321−337.
(11) Ren, J.; Chaires, J. B. Sequence and structural selectivity of nucleic acid binding ligands. *Biochemistry* **1999**, *38*, 16067−16075.
(12) Ren, J.; Chaires, J. B. Rapid screening of structurally selective ligand binding to nucleic acids. *Methods Enzymol* **2001**, *340*, 99−108.
(13) Chaires, J. B. A competition dialysis assay for the study of structure-selective ligand binding to nucleic acids. In *Current Protocols in Nucleic Acid Chemistry*; John Wiley & Sons: New York, 2002; p 8.3.1−8.3.8.
(14) Nguyen, B.; Tardy, C.; Bailly, C.; Colson, P.; Houssier, C.; et al. Influence of compound structure on affinity, sequence selectivity, and mode of binding to DNA for unfused aromatic dications related to furamidine. *Biopolymers* **2002**, *63*, 281−297.
(15) Das, B. P.; Boykin, D. W. Synthesis and antiprotozoal activity of 2,5-bis(4-guanylphenyl)furans. *J. Med. Chem.* **1977**, *20*, 531−536.
(16) Boykin, D. W.; Kumar, A.; Xiao, G.; Wilson, W. D.; Bender, B. C.; et al. 2,5-bis[4-(N-alkylamidino)phenyl]furans as anti-*Pneumocystis carinii* agents. *J. Med. Chem.* **1998**, *41*, 124−129.
(17) Das, B. P.; Boykin, D. W. Synthesis and antiprotozoal activity of 2,5-bis(4-guanylphenyl)thiophenes and -pyrroles. *J. Med. Chem.* **1977**, *20*, 1219−1221.
(18) Francesconi, I.; Wilson, W. D.; Tanious, F. A.; Hall, J. E.; Bender, B. C.; et al. 2,4-Diphenyl furan diamidines as novel anti-*Pneumocystis carinii* pneumonia agents. *J. Med. Chem.* **1999**, *42*, 2260−2265.
(19) Wilson, W. D.; Tanious, F. A.; Mizan, S.; Yao, S.; Kiselyov, A. S.; et al. DNA triple-helix specific intercalators as antigene enhancers: Unfused aromatic cations. *Biochemistry* **1993**, *32*, 10614−10621.
(20) Wilson, W. D.; Mizan, S.; Tanious, F. A.; Yao, S.; Zon, G. The interaction of intercalators and groove-binding agents with DNA triple-helical structures: The influence of ligand structure, DNA backbone modifications and sequence. *J. Mol. Recognit.* **1994**, *7*, 89−98.
(21) Jorgensen, W. L.; Chandrasekhar, J.; Madura, J. D.; Impey, R. W.; Klein, M. L. Comparison of simple potential functions for simulating liquid water. *J. Chem. Phys.* **1983**, *79*, 926−935.
(22) Bayly, C. I.; Cieplak, P.; Cornell, W.; Kollman, P. A. A well-behaved electrostatic potential based method using charge restraints for deriving atomic charges: The RESP model. *J. Phys. Chem.* **1993**, *97*, 10269−10280.
(23) Cornell, W. D.; Cieplak, P.; Bayly, C. I.; Gould, I. R.; Merz, K. M.; et al. A second generation force field for the simulation of proteins, nucleic acids, and organic molecules. *J. Am. Chem. Soc.* **1995**, *117*, 5179−5201.
(24) Case, D. A.; Pearlman, D. A.; Caldwell, J. W.; Cheatham, T. E., III.; Ross, W. S.; et al. *AMBER*, version 5.0; University of California: San Francisco.
(25) Hamelberg, D.; Williams, L. D.; Wilson, W. D. Influence of the dynamic positions of cations on the structure of the DNA minor groove: Sequence-dependent effects. *J. Am. Chem. Soc.* **2001**, *123*, 7745−7755.
(26) Hamelberg, D.; Williams, L. D.; Wilson, W. D. Effect of a neutralized phosphate backbone on the minor groove of B-DNA: Molecular dynamics simulation studies. *Nucleic Acids Res.* **2002**, *30*, 3615−3623.
(27) Ryckaert, J. P.; Ciccotti, G.; Berendsen, H. J. C. Numerical integration of the Cartesian equations of motion of a system with comstraints: Molecular dynamics of *n*-alkanes. *J. Comput. Phys.* **1977**, *23*.
(28) Essmann, U.; Perera, L.; Berkowitz, M. L.; Darden, T. A.; Lee, H.; et al. A Smooth Particle Mesh Ewald Methodology. *J. Chem. Phys.* **1995**, *103*, 8577−8593.
(29) Cleveland, W. S. *The Elements of Graphing Data*; Wadsworth Advanced Books and Software: Monterey, CA, 1985.
(30) Chaires, J. B.; Ren, J.; Henary, M.; Zegrocka, O.; Bishop, G. R.; et al. Triplex selective 2-(2-naphthyl)quinoline compounds: Ori-

gins of affinity and new design principles. *J. Am. Chem. Soc.* **2003**, *125*, 7272−7283.
(31) Trent, J. O.; Clark, G. R.; Kumar, A.; Wilson, W. D.; Boykin, D. W.; et al. Targeting the minor groove of DNA: Crystal structures of two complexes between furan derivatives of berenil and the DNA dodecamer d(CGCGAATTCGCG)$_2$. *J. Med. Chem.* **1996**, *39*, 4554−4562.
(32) Sinden, R. R. *DNA Structure and Function*; Academic Press: San Diego, 1994; 398.
(33) Trent, J. O. Advances in DNA Molecular Modeling. An Update. *Methods Enzymol.* **2001**, *340*, 290−326.
(34) Jenkins, T. C. Targeting multi-stranded DNA structures. *Curr. Med. Chem.* **2000**, *7*, 99−115.
(35) Mergny, J. L.; Duval-Valentin, G.; Nguyen, C. H.; Perrouault, L.; Faucon, B.; et al. Triple helix-specific ligands. *Science* **1992**, *256*, 1681−1684.

JM049491E